Sensors and Materials, Vol. 9, No. 2 (1997) 083–095
MYU Tokyo

S & M 0275

Structure and Impedance Behaviors of Thick Pt/YBCO Electrode Film on YSZ Substrate in (O_2 + NO) Mixture

Takeshi Nagai, Kenzo Ohji, Akio Fukuda and Takahiro Umeda

Yamatokoriyama Laboratory, Research Institute of Innovative Technology for the Earth,
Home Appliance Research Laboratory, Matsushita Electric Industrial Co., Ltd.,
Tsutsui, Yamatokoriyama, Nara 639-11, Japan

(Received November 6, 1995; accepted November 5, 1996)

Key words: thick Pt/YBCO film, YSZ substrate, impedance behavior, XRD pattern, (O_2 + NO) atmosphere

A thick Pt/YBCO [mixture of Pt and $YBa_2Cu_3O_x$(YBCO)] electrode film was fired on a YSZ substrate. The impedance behaviors of the Pt/YBCO film were measured in the temperature range of 400–550°C in various (O_2 + NO) atmospheres diluted with He. The structure of the Pt/YBCO film was also studied by means of XRD analysis. As a result, the electrode impedance was found to be very sensitive to the O_2 concentration in O_2 atmosphere. This high sensitivity may be attributed to the involvement of lattice oxygen atoms of orthorhombic YBCO in the cathodic electrode reaction. The electrode impedance was also very sensitive to a small NO concentration (0.05 – 0.5%) in (10%O_2 + NO) atmospheres. This high sensitivity to the NO concentration may be attributed to the growth of $Ba(NO_3)_2$ in (10%O_2 + NO) atmosphere and the involvement of lattice oxygen atoms of $Ba(NO_3)_2$ in the cathodic electrode reaction.

1. Introduction

Since nitrogen oxide (NO_x: NO and NO_2) causes air pollution such as acid rain and photochemical smog, as well as damage to human health, there have been many studies on ways to reduce the level of NO_x exhausted from combustion apparatus. Selective catalytic reduction using NH_3 has already been applied to large-scale industrial plants such as thermal power stations and garbage furnaces. However, there has been no success in the

development of a means of reduction suitable for mobile generators such as automobiles and small generators such as domestic gas or oil stoves. Catalytic reduction[1-3] and electrochemical reduction[4-7] using solid electrolytes have been studied as typical means of reducing NO_x in such areas. One of the most difficult problems in NO_x reduction is that only a small amount can be reduced in an O_2-rich atmosphere.

We have recently studied the impedance behaviors of an element comprising a thick Pt/YBCO [mixture of Pt and YBa_2Cu_3Ox (YBCO)] electrode film fired on a YSZ (8 mol% Y_2O_3 stabilized ZrO_2) substrate using by a conventional firing technique. We found that the impedance behavior of the element is very sensitive to a small amount of NO (0.05–0.5%) even in an atmosphere containing a large amount of O_2 (10%). This high sensitivity suggests a possibility of NO_x reduction in O_2-rich atmosphere. The Pt/YBCO film was selected for the following reasons: (1) Not only is YBCO a high-temperature superconducting material, it is also a preferred chemisorption material[8] of NO in O_2-rich atmosphere; and (2) Pt is one of the most appropriate materials for use as an electrode on the YSZ substrate.

In this paper, we describe the composition, structure and impedance behaviors of Pt/YBCO film fired on YSZ substrate in various (O_2 + NO) atmospheres in the temperature range of 400–550°C.

2. Experimental

A mixture paste was prepared by adding YBCO powder of 1–3 μm in diameter to a conventional Pt paste to make a YBCO weight concentration of 20%. After the mixture paste was printed on the YSZ substrate (10 mm × 10 mm × 0.35 mm^t) and dried at 100°C, a thick Pt/YBCO electrode film was prepared by firing the dried film at 820°C for 10 min in air. A cross section of the construction is shown in Fig. 1 together with the impedance measuring method. The counter (CE) and working (WE) electrodes were composed of thick Pt and Pt/YBCO film with areas of 48 mm^2 (6 mm × 8 mm). Their thicknesses were 10–15 μm and 15–20 μm, respectively. The reference electrode (RE) was composed of a thick Pt film with an area of 8 mm^2 (1 mm × 8 mm) and a thickness of 10–15 μm. The thick

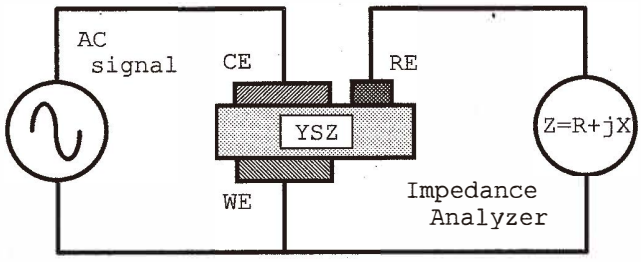

Fig. 1. Cross-sectional element construction.

Pt film was also fired at 820°C for 10 min in air using the conventional Pt paste. A Pt wire (0.1 mm in diameter) was connected to each electrode.

The element was placed in a quartz tube and its impedance was measured at a gas flow of 200 cc/min in the temperature range of 400–550°C. Various gas compositions were used by mixing He gas, O_2 gas and NO gas diluted with He. Impedance measurements were performed using a Solarton Impedance Analyzer (SI1260). An AC signal voltage of ±5 mVrms was applied between CE and WE in the frequency range of 0.1 Hz–40 kHz. Impedances between RE and WE were measured.

A high-temperature XRD apparatus (Mac-Science, MXP[3]) was employed to evaluate the composition and structure of the Pt/YBCO film. The apparatus was equipped with a Pt heater and external lead terminals in a small chamber sealed from the surroundings. The element was placed on the Pt heater and its Pt lead wires were connected to the terminals. The XRD patterns were then measured under conditions similar to those of the impedance measurements with or without DC current flow between CE and WE. Measurements were performed with $CuK_{\alpha 1}$ radiation (40 kV, 40 mA) using steps of 0.02° and 1°/min.

3. Composition and Structure of Pt/YBCO Film during Firing Process

A SEM micrograph of the Pt/YBCO film is shown in Fig. 2 in comparison with that of the Pt film. The surface structures of the two films were similar in terms of porosity. The electrical resistance of the former was about 2 Ω/□ at room temperature, which was over one order of magnitude larger than that of the latter (about 0.1 Ω/□). Firing of a single YBCO electrode film without Pt was also attempted on the YSZ substrate under the same firing conditions as those described above. However, the thus-prepared single YBCO film was not suitable for use as an electrode because of its very high electrical resistance (above 2 MΩ/□).

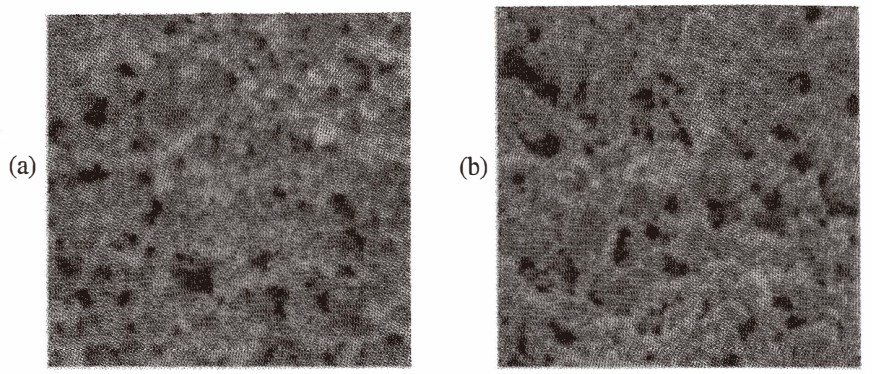

Fig. 2. SEM micrographs of the electrode film (× 1000). (a) Pt/YBCO film, (b) Pt film.

The effects of firing temperature on the composition and structure of the Pt/YBCO film were evaluated by XRD analyses as follows. After the mixture paste was printed on the YSZ substrate, the printed film was dried at about 100°C in air. The dried film was then placed on the Pt heater in the XRD apparatus and XRD patterns were measured in an air flow of 200 cc/min and in the following temperature order: room temperature(RT) → 500°C → 600°C → 700°C → 800°C → 900°C → 500°C → RT. The crystal structure of YBCO was reported to change from orthorhombic to tetragonal phase with increasing temperature.[9,10] During this phase change, one of the most characteristic changes was the inversion of intensity for the set of reflection near 2θ~32.7° at room temperature. Figure 3 shows typical XRD patterns of the Pt/YBCO film between $2\theta = 30°$ and 34° in comparison with those of the single YBCO film.

Strong peaks of the YBCO phase and weak peaks of unknown phase were observed in the XRD patterns of the single YBCO film. The orthorhombic phase began to transit gradually to the tetragonal phase at temperatures above 600°C and the phase transition was completed below 800°C. After the specimen was cooled to room temperature, the XRD patterns were measured again. In comparing the initial and final XRD patterns measured at room temperature, a decease in peak intensity near 2θ~32.7° and the appearance of a weak peak of unknown phase were observed in the final XRD pattern. The findings suggest that the YBCO phase decomposes slightly during the heat treatment.

The peaks of the YBCO phase in the XRD patterns of the Pt/YBCO film were similar to those of the single YBCO film at temperatures below 800°C. However, the XRD pattern was quite different from that of the single YBCO film at 900°C. Peaks of the YBCO phase almost completely disappeared and only peaks of an unknown phase were observed. Following this measurement at 900°C, no peaks of the YBCO phase and only peaks of the unknown phase were observed in the subsequent measurements at lower temperatures. These results indicate that the YBCO phase decomposed completely during the heat treatment at 900°C. In addition, in the initial measurement at temperatures below 800°C, the orthorhombic phase began to transit to the tetragonal phase above 600°C and the phase transition was completed below 700°C. This phase transition appeared to proceed more rapidly at a lower temperature than that of the single YBCO film. The complete decomposition of the YBCO phase and the lower phase transition temperature suggest an interaction between Pt and YBCO particles in the Pt/YBCO film.

The Pt/YBCO film fired at 820°C showed strong peaks of Pt phase, and weak peaks of YBCO and some weak peaks of unknown phase were observed in the XRD pattern measured at room temperature in the wide range of 2θ (20°~80°). This result indicates that the Pt/YBCO film is the mixture of Pt, YBCO and unknown phase. However, the film fired at 920°C showed strong peaks of Pt, no peaks of YBCO and weak peaks of unknown phase. This result indicates that the film contains no YBCO phase.

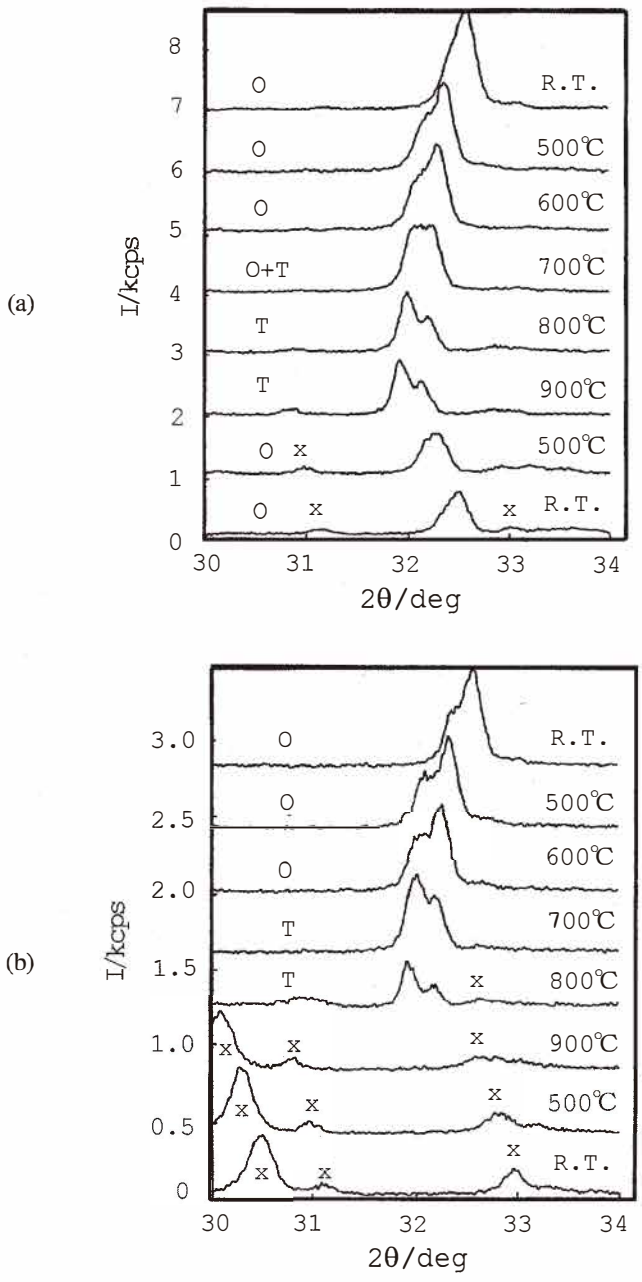

Fig. 3. XRD patterns obtained at various temperatures (O: orthorhombic phase, T: tetragonal phase, x: peaks of unknown phase). (a) YBCO film, (b) Pt/YBCO film.

4. Impedance Behaviors

Impedance behaviors of the Pt/YBCO film and of the Pt film were measured and compared. The Pt/YBCO and Pt films were fired at 820°C for 10 min in air as the working electrodes. Measurements were performed at 400–550°C in various (O_2 + NO) atmospheres. Typical results are shown in Figs. 4 and 5. Since the impedance behavior in the lower frequency range reflects an electrode reaction, these figures show mainly the impedance plots below 10 kHz.

In various O_2 atmospheres (Fig. 4), the impedance plots of the Pt film formed a small portion of a semi-circle, even at 550°C. In other words, the impedance plots of the Pt film were independent of O_2 concentration. Conversely, the Pt/YBCO film showed strong O_2 concentration dependence even at 450°C in its impedance plots which formed large portions of semi-circles. Above 500°C, the plots showed almost full semi-circles. The electrode impedances of the Pt/YBCO film were over one order of magnitude lower than those of the Pt film in various O_2 atmospheres.

In various (10%O_2 + NO) atmospheres (Fig. 5), the impedance plots of the Pt film showed considerable NO concentration dependence even at 450°C. However, as in O_2 atmospheres, the impedance plots of the Pt/YBCO film showed stronger NO concentration dependence than those of the Pt film and the electrode impedances were more than one order of magnitude lower than those of the Pt film in various (10%O_2 + NO) atmospheres.

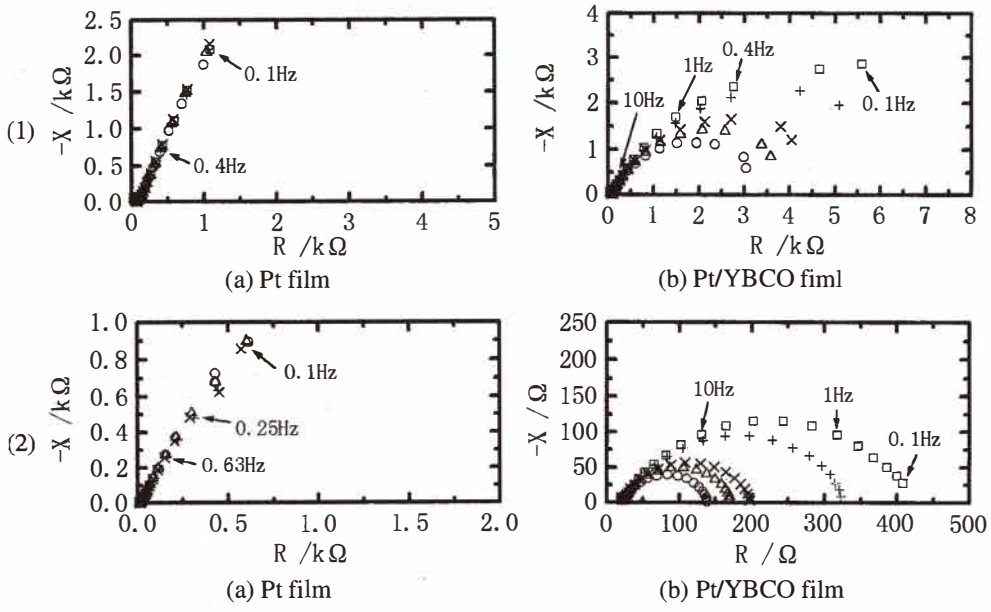

Fig. 4. Typical impedance plots in O_2 atmospheres (O_2 concentration: □, 0.05%; +, 0.5%; ×, 5%; △, 10%; ○, 20%). (1) 450°C, (2) 550°C.

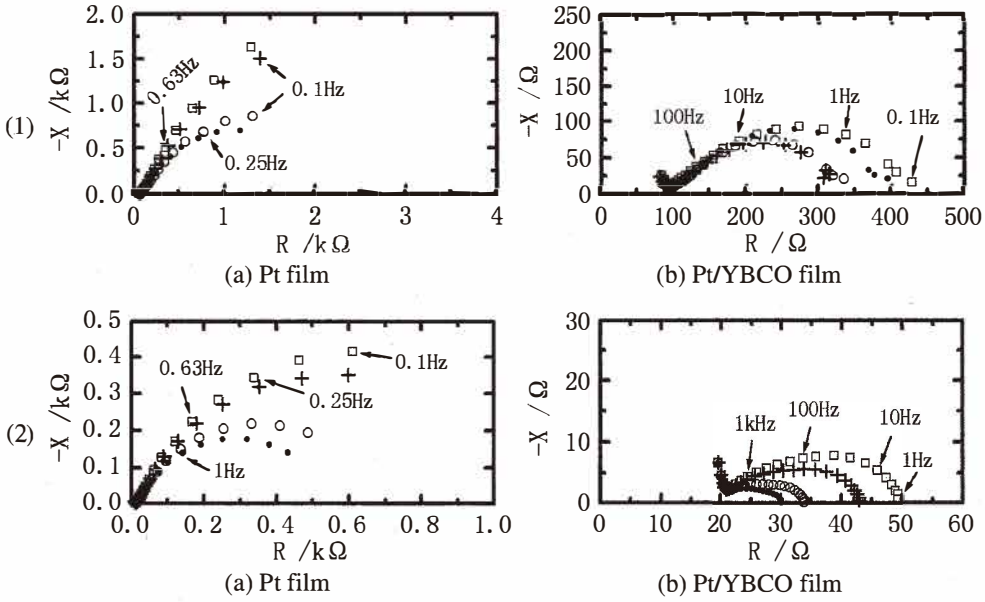

Fig. 5. Typical impedance plots in ($10\%O_2$ + NO) atmospheres (NO concentration: □, 0.05%; +, 0.1%; ○, 0.3%; ●, 0.5%). (1) 450°C, (2) 550°C.

In comparing the impedance plots of the Pt/YBCO film in O_2 atmospheres and those in ($10\%O_2$ + NO) atmospheres, we find that the electrode impedance was apparently several times lower in the latter atmospheres. For example, the electrode resistances were about 4 kΩ and about 150 Ω at 450°C and 550°C, respectively, in the $10\%O_2$ atmosphere. Conversely, they were about 350 Ω and about 30 Ω at 450°C and 550°C, respectively, in the ($10\%O_2$ + 0.05%NO) atmosphere. These findings suggest that the Pt/YBCO film was very sensitive to a small amount of NO in an O_2-rich atmosphere and that the sensitivity appeared to decrease with increasing temperature.

5. Effects of Atmosphere and DC Current on the Structure of Pt/YBCO Film

The XRD patterns of the Pt/YBCO film were measured at 450°C in He, ($10\%O_2$ + 2%NO) and $10\%O_2$ atmosphere in that order with or without DC current flow. In addition, since the Pt/YBCO film was formed at 1 mm from the inside edge of the YSZ substrate, X-rays were incident on the edge of the YSZ substrate. As a result, peaks of ZrO_2 were also observed. In the following figures, the XRD patterns between $2\theta = 28°$ and 31° were eliminated because of a very strong peak of the ZrO_2 phase near $2\theta = 29.9°$.

5.1 *XRD patterns in He atmosphere*

Typical XRD patterns of the Pt/YBCO film are shown in Fig. 6. The O_2 concentration in He atmosphere was estimated to be below 70–80 ppm. The XRD pattern was initially measured without DC current flow. The intensity of the set of peaks observed near $2\theta = 32.7°$ suggests that the Pt/YBCO film contains the orthorhombic YBCO phase.

After DC current flow of 7.5 mA/cm^2 was maintained for 10 min in He atmosphere before the measurements, an XRD pattern was measured during the DC current flow. In this measurement, the Pt/YBCO film was used as the anode and the Pt film was used as the cathode. The XRD pattern was almost identical to that measured initially without DC current flow. Next, an XRD pattern was obtained under the same conditions as the above but using the Pt/YBCO film as the cathode and the Pt film as the anode. The intensity of the set of peaks near $2\theta = 32.7°$ was almost identical to that of the single YBCO film measured at 700°C in air. This finding indicates the coexistance of the orthorhombic and tetragonal phases in the Pt/YBCO film at a lower temperature of 450°C. From these results, it is apparent that lattice oxygen atoms of the orthorhombic YBCO phase were involved in the cathodic electrode reaction.

In the cathodic electrode reaction, lattice oxygen atoms in YBCO [O(YBCO)] may move on the Pt particle surface as adsorbed oxygen atoms [O_{ad}(Pt)] and the O_{ad}(Pt) must transit through Pt/YSZ/atmosphere three phase boundaries (tpb) into the YSZ substrate as O^{--} ions [O_O^X(YSZ)], as shown in Fig. 7. This cathodic electrode reaction can be represented as follows:

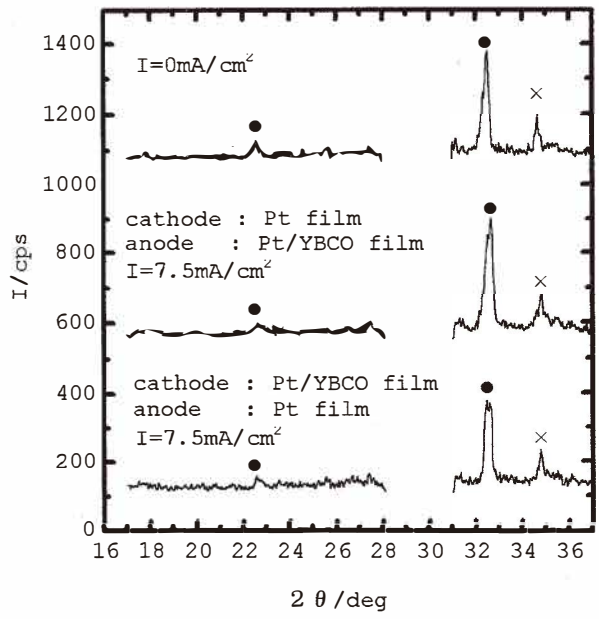

Fig. 6. XRD patterns in He atmosphere at 450°C (●: YBCO, ×: ZrO_2).

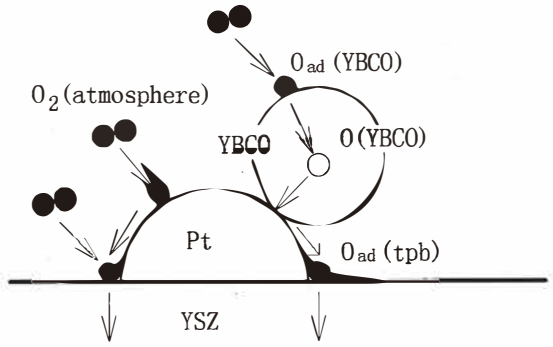

Fig. 7. Reaction mechanism of Pt/YBCO film with atmospheric O_2 molecules in O_2 atmosphere.

$$O(YBCO) \rightarrow O_{ad}(Pt) \quad (1)$$

$$O_{ad}(Pt) \rightarrow O_{ad}(tpb) \quad (2)$$

$$O_{ad}(tpb) + V_O(YSZ) + 2e \rightarrow O_O^X(YSZ) + V_{ad}(tpb) \quad (3)$$

where $O_{ad}(tpb)$, $V_O(YSZ)$ and $V_{ad}(tpb)$ denote adsorbed oxygen atom on the tpb, oxygen vacancy in YSZ and vacant adsorption site on the tpb, respectively. Equation (1) implies that O(YBCO) atoms move on the Pt surface via the contacts between the Pt and YBCO particles. Equations (2) and (3) are conventional cathodic electrode reactions in the Pt film.[11] The consumed O(YBCO) atoms in eq. (1) may be supplied from atmospheric O_2 molecules as follow:

$$O_2(atmosphere) \rightarrow 2O_{ad}(YBCO) \quad (4)$$

$$O_{ad}(YBCO) \rightarrow O(YBCO) \quad (5)$$

where O_2 (atmosphere) and O_{ad} (YBCO) denote O_2 molecules in the atmosphere and dissociated oxygen atoms on the YBCO surface, respectively. Equations (1), (4) and (5) are expected to be also applied in (He + O_2) atmosphere. The high sensitivity of the Pt/YBCO film to O_2 concentration as observed from the impedance behaviors is attributed to these reactions.

In addition, the reason why eq. (1) proceeds is unknown. However, the reaction rate in eq. (1) appears to be faster than that in the reaction in which O(YBCO) transit directly into the YSZ substrate as O_O^X(YSZ) through YBCO/YSZ/atmosphere tpb. Needless to say, O_2 (atmosphere) molecules may be also dissociated on the Pt surface and the dissociated oxygen atoms [O_{ad}(Pt)] transit into the YSZ substrate. These conventional reactions in the Pt film proceed together with those represented by eqs. (1), (4) and (5), which are characteristic of the Pt/YBCO film.

5.2 *XRD patterns in (10%O_2 + 2%NO) atmosphere*

Typical XRD patterns of the Pt/YBCO film are shown in Fig. 8 when the Pt/YBCO film was used as a cathode at 450°C with or without DC current flow in (10%O_2 + 2%NO) atmosphere. Two characteristic results have been found.

Firstly, the intensity of the YBCO peaks near 2θ = 32.7° was greatly reduced. However, the Pt/YBCO film showed apparent peaks of orthorhombic-like phase even under a DC current flow of 7.5 mA/cm^2. Considering the phase transition of YBCO under the same DC current flow in He atmosphere, this result supports the supply of oxygen atoms from atmospheric O_2 or NO molecules to the orthorhombic YBCO.

Secondly, new peaks of $Ba(NO_3)_2$ were observed near 2θ = 18.7°, 21.6° and 36.4° even without DC current flow. These peaks exhibited almost no change during the DC current flow. This finding suggests that $Ba(NO_3)_2$ grew with no relation to the DC current. Since Pt is a strong oxidizing catalyst, it is reasonable that NO_2 is formed near the Pt particles in the Pt/YBCO film in (10%O_2 + 2%NO) atmosphere. Since NO_2 molecules were easily adsorbed, the reaction of adsorbed NO_2 molecules with YBCO resulted in the growth of $Ba(NO_3)_2$, as follows:

$$2NO(\text{atmosphere}) + O_2(\text{atmosphere}) \rightarrow 2NO_2(\text{atmosphere}) \quad (6)$$

$$2NO_2(\text{atmosphere}) \rightarrow 2NO_{2ad}(\text{YBCO}) \quad (7)$$

$$2NO_{2ad}(\text{YBCO}) + Ba(\text{YBCO}) + 2O(\text{YBCO}) \rightarrow Ba(NO_3)_2(\text{YBCO}) \quad (8)$$

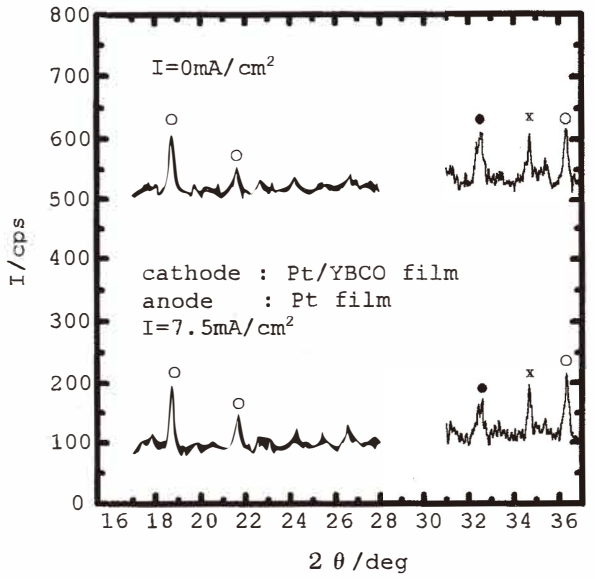

Fig. 8. X RD patterns in (10%O_2 + 2%NO) atmosphere at 450°C (●: YBCO, ×: ZrO_2, ○: $Ba(NO_3)_2$).

where NO(atmosphere), NO_2(atmosphere), NO_{2ad}(YBCO), Ba(YBCO) and $Ba(NO_3)_2$(YBCO) denote the atmospheric NO molecules, the atmospheric NO_2 molecules, the adsorbed NO_2 molecules on the YBCO surface, lattice Ba atoms in YBCO and the grown $Ba(NO_3)_2$ molecules on the YBCO surface, respectively. This $Ba(NO_3)_2$ growth decomposes YBCO and results in the reduced intensity of YBCO peaks.

XRD patterns were also measured in ($10\%O_2$ + 0.5%NO) atmosphere using another element. In this case, the intensity of YBCO peaks was not greatly reduced and peaks of $Ba(NO_3)_2$ were very weak. This result suggests that the decrease in YBCO peak intensity and the growth of $Ba(NO_3)_2$ depend strongly on the NO concentration. Considering that $Ba(NO_3)_2$ is expected to grow at NO concentrations below 0.5% in O_2-rich atmosphere, the high sensitivity of the Pt/YBCO film to lower NO concentration in O_2-rich atmosphere as observed from the impedance behaviors may be attributed to the growth of $Ba(NO_3)_2$. In addition, the intensity of the new peaks of $Ba(NO_3)_2$ did not change during the DC current flow. This will be discussed in the following section.

5.3 *XRD patterns in $10\%O_2$ atmosphere*

After XRD patterns of the Pt/YBCO film were measured in ($10\%O_2$ + 2%NO) atmosphere, those of the same Pt/YBCO film were measured in $10\%O_2$ atmosphere at 450°C. Typical XRD patterns are shown in Fig. 9. When the Pt/YBCO film was used as an anode or without DC current flow, the patterns were almost the same as those measured

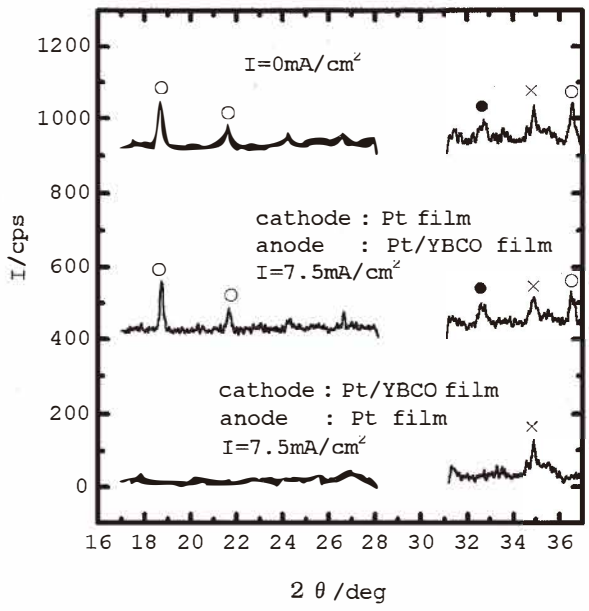

Fig. 9. XRD patterns in $10\%O_2$ atmosphere at 450°C (●: YBCO, ×: ZrO_2, ○: $Ba(NO_3)_2$).

in (10%O_2 + 2%NO) atmosphere. However, when the Pt/YBCO film was used as a cathode, the intensity of $Ba(NO_3)_2$ peaks was apparently reduced during DC current flow of 7.5 mA/cm^2. This result suggests that the oxygen atoms in $Ba(NO_3)_2$ may be involved in the cathodic electrode reaction.

Since eqs. (1)–(5) may be applied in (He + O_2) atmosphere, as described before, O(YBCO) atoms are consumed in the cathodic electrode reaction. Needless to say, many consumed O(YBCO) atoms may be supplied from atmospheric O_2 molecules in (He + O_2) atmosphere. However, although the detailed processes are unknown, some consumed O(YBCO) atoms appear to be supplied from lattice oxygen atoms [$O(Ba(NO_3)_2)$] of $Ba(NO_3)_2$ according to eq. (9), as shown in Fig. 10. As a result, $Ba(NO_3)_2$ may decompose and its peak intensity may be reduced.

$$O[Ba(NO_3)_2] \rightarrow O(YBCO) \tag{9}$$

Equation (9) may be expected to proceed also in (O_2 + NO) atmosphere. However, decomposed $Ba(NO_3)_2$ molecules may react with atmospheric NO_2, and $Ba(NO_3)_2$ may be formed again. As a result, its peak intensity does not change even during DC current flow in (O_2 + NO) atmosphere.

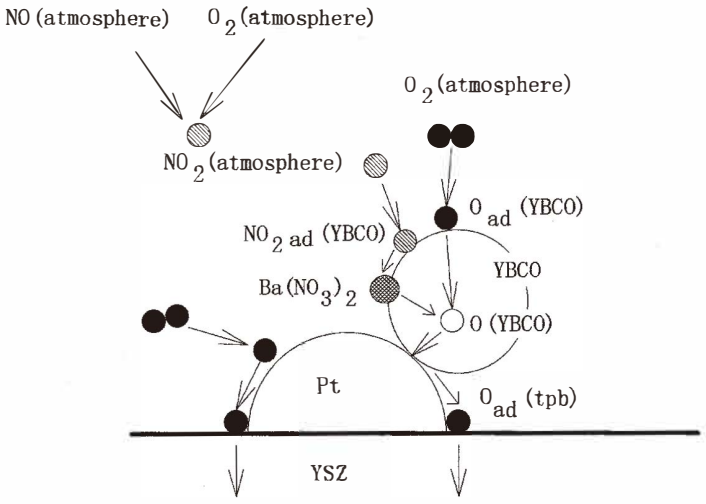

Fig. 10. Reaction mechanism of Pt/YBCO film with atmospheric NO molecules in (O_2 + NO) atmosphere.

6. Conclusion

It was found that Pt/YBCO film on YSZ substrate was very sensitive to both O_2 and NO concentrations in (He + O_2 + NO) atmosphere. The sensitivity to O_2 molecules may be attributed to the involvement of O(YBCO) atoms in the cathodic electrode reaction. The sensitivity to NO molecules may be attributed to the growth of $Ba(NO_3)_2$ and the involvement of $O[Ba(NO_3)_2]$ atoms in the cathodic electrode reaction.

The element comprising Pt/YBCO film on YSZ substrate has potential for NO_x sensor application[12] and for use as NO_x decomposition devices. The decomposition has been confirmed experimentally in (He + O_2 + NO) atmosphere and the results will be reported in the near future.

Acknowledgment

We would like to thank Professor A. Hikaki of Osaka University for his helpful discussions. This work was supported by RITE (Research Institute of Innovative Technology for the Earth).

References

1 S. Sato, Y. Yu-u, H. Yahiro, N. Mizuno and M. Iwamoto: Appl. Catal. **L1** (1991) 70.
2 H. Yasuda, N. Mizuno and M. Misono: J. Chem. Soc. Commun. (1990) 1094.
3 H. Hamada, Y. Kintaichi, M. Sasaki, T. Itoh and M. Tabata: Appl. Catal. **L1** (1990) 64.
4 S. Pancharatnam, R. A. Huggins and D. M. Mason: J. Electrochem. Soc. **122** (1975) 869.
5 T. M. Gur and R. A. Huggins: J. Electrochem. Soc. **126** (1979) 1067.
6 M. M. Wright and J. E. Smith: Intersoc. Energy Convers. Eng. Conf. **27** (1992) 4321.
7 T. Hibino, A. Masegi and H. Iwahara: Shokubai **36** (1994) 448.
8 K. Tabata, H. Fukuda, S. Kohiki, N. Mizuno and M. Misono: Chem. Lett. (1988) 799.
9 P. K. Gallagher, H. M. O'Brayan, S. A. Sunshine and D. W. Murphy: Mat. Res. Bull. **22** (1987) 995.
10 K. Kishio, J. Shimoyama and T. Hasegawa: Jpn. J. Appl. Phys. **26** (1987) L1228.
11 D. Y. Wang and A. S. Nowick: J. Electrochem. Soc. **126** (1979) 1155.
12 T. Nagai, K. Ohji, A. Fukuda and T. Umeda: Technical Digest of the 13th Sensor Symposium (1995) 69.